To Appear: **Robotica Journal**, 2001:

Pin Design for Part Feeding

Tao Zhang[†] Ken Goldberg[*] Gordon Smith[✧]
Robert-Paul Berretty[♣] Mark Overmars[♠]
UC Berkeley, Utrecht University, and UNC Chapel Hill

Abstract -- Industrial parts can be fed (oriented) using a sequence of fixed horizontal pins to topple the parts as they move past on a conveyor belt. We give an algorithm for designing a sequence of such pins for a given part. Given the *n*-sided convex polygonal projection of a part, its center of mass and frictional coefficients, our $O(n^2)$ algorithm computes the *toppling graph*, a new data structure that explicitly represents the mechanics of toppling, rolling, and jamming. We verify the toppling graph analysis with experiments. Our $O(n^{3n})$ design algorithm uses the toppling graph to design a sequence of pin locations that will cause the part to emerge in a unique orientation or to determine that no such sequence exists.

Index Terms -- Manufacturing, Assembly, Part Feeding, Motion Planning.

I. Introduction

To facilitate rapid setup and changeover of industrial assembly lines, CAD/CAM software can analyze part geometry and mechanics to assist in the design of components such as grippers, fixtures, and part feeders. In this paper we focus on a class of part feeders that uses a sequence of horizontal pins to topple a stream of identical parts as they move past on a conveyor belt. Pin heights must be designed for a given part and set of frictional coefficients. Manual analysis is complex and tedious; in this paper we describe an automated design algorithm based on the *toppling graph*, a new data structure that compactly represents the mechanics of toppling, rolling, and jamming. We give an algorithm for computing this graph, and then use the graph in a second algorithm that designs a sequence of pins or determines that no such sequence exists.

The input to our algorithm is the *n*-sided convex polygonal projection of the part, its center of mass, and the coefficients of frictional between the part and the conveyor belt and the part and the pins. Gravity forces each part to arrive at the first pin in one of *n* stable orientations. For each stable orientation, we find a range of critical pin heights that will cause the part to rotate into the next stable orientation without jamming. We then design an arrangement of pins that will work for all stable part orientations.

We develop a set of functions to represent the mechanics of toppling. Lynch[1,2] was the first to formalize mechanical conditions for toppling and to study pin sequences for part feeding. Here, we extend Lynch's analysis and develop a geometric design algorithm.

We define geometric functions that map from part orientation to distance: $S^1 \rightarrow \Re^+$. These functions describe the height of vertices and critical jamming conditions as the part rotates. These functions are defined on planar slices of configuration space (C-space) and are generalizations of the radius and width functions[5]. The *toppling graph* is a new data structure that combines these functions to facilitate identification of critical pin heights.

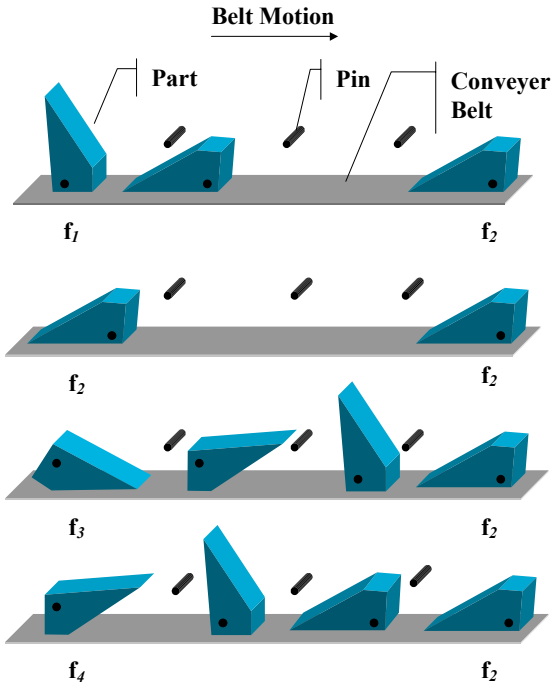

Figure 1. This sequence of 3 pins (coming out of figure) will orient the polygonal part as it moves from left to right: all initial part orientations are rotated to the same final orientation.

II. Related Work

Erdmann and Mason[3] were the first to develop sensorless manipulation planning algorithms. They analyze the problem of orienting a given part by tilting a planar tray, causing the part to make contact with tray walls in a specific sequence of directions. They identify critical tilting directions and develop a complete algorithm to find tilt sequences by searching the finite tree of all sequences. They showed that sensing is not required to guarantee a unique final orientation, hence the term: *sensorless manipulation*. Brost[4] developed analytical methods for describing the interaction between a pair of polygonal objects and gave algorithms for constructing forbidden regions (obstacles) in the configuration-space (C-space). Goldberg[5] analyzed sequences of parallel-jaw grasping operations that will orient polygonal parts without sensors. He proved that such a sequence exists for any polygonal part and gave an $O(n^2)$ algorithm for finding optimal sequences. Abell and Erdmann[6] studied how a planar polygon can be rotated in a gravitational field while stably supported by two frictionless contacts. Zumel and Erdmann[7,8] analyzed nonprehensile manipulation using two palms jointed at a central hinge and developed sensorless sequences to orient parts.

Lozano-Perez[9] treated the design of part feeding devices as dual to motion planning. He described feeders using C-space. In this paper, we develop a C-space formulation for the mechanics of pins. Natarajan[10] gave a computational abstraction for part-feeding devices. Given k transfer functions, $f_1, f_2, \ldots, f_k$, on a finite set $\boldsymbol{S}$, Natarajan showed that f_0, if it exists, can be found in time $O(kn^4)$ such that $|f_0(\boldsymbol{S})| = |\{f_0(v) \mid v \in \boldsymbol{S}\}| = 1$, where f_0 is a composite of the f_i's and n is the size of $\boldsymbol{S}$. Caine[11] represented part interactions as motion constraints in C-space, and developed a set of computational tools for computer aided design of vibratory bowl feeder tracks. Christiansen *et al.*[12] used genetic algorithms to generate vibratory feeder tracks. Berkowitz and Canny[13] used dynamic simulation to test candidate feeder tracks.

Many part feeding devices have been studied. Peshkin and Sanderson[14] analyzed the problem of orienting parts on a conveyor belt with a sequence of fixed planar fences. They discretized the range of fence angles to search for sequences of fences. Wiegley *et al.*[15] added curved tips to the fences to insure that the transfer functions are deterministic and gave a complete algorithm to compute the shortest sequence of fences. Berretty *et al.*[16] gave a polynomial-time algorithm to find such a sequence for any polygonal part. Gudmundsson and Goldberg[17] derived optimal conveyor belt velocities using a queuing model. Akella *et al.*[18] showed that a one-joint robot can orient parts by sweeping a planar fence over the conveyor belt.

Bicchi and Sorrentino[19] analyzed the mechanics of 3D rolling with a pair of parallel jaws. Berretty *et al.*[20] studied vibratory feeder traps and gave algorithms to design traps based on part geometry. Blind *et al.*[21] designed a "*Pachinko*"-like device to orient polygonal parts in the vertical plane using a grid of retractable pins that are programmed to bring the part to a desired orientation as it falls.

Our work is also motivated by recent research in toppling manipulation. Zhang and Gupta[22] analyzed how parts are reoriented as they fall down a series of steps. Yu *et al.*[23] showed how to estimate the mass properties of parts by detecting toppling with a force sensor. Lynch[1,2] derived a set of graphical toppling conditions based on part geometry, center of mass, and coefficients of friction at the support and toppling contacts.

III. Problem Definition

We consider a stream of well-separated identical parts traveling horizontally along a conveyor belt. As parts come into contact with horizontal cylindrical pins, parts are caused to rotate in the plane orthogonal to the pins until they fall into a new stable orientation on the conveyor belt. We assume that pins are fixed and rigid, inertial forces are negligible, and that part geometry and center of mass are known exactly.

The input of our algorithm is a list of vertices defining an n-sided convex polygon, its center of mass (COM), and coefficients of friction, μ_t and μ_p: between the part and belt and between the part and pin respectively. The output of our algorithm is a (possibly empty) range of critical pin heights for the part at each of its stable orientations. A pin at a critical pin height is guaranteed to topple the part from one stable orientation to the next without jamming.

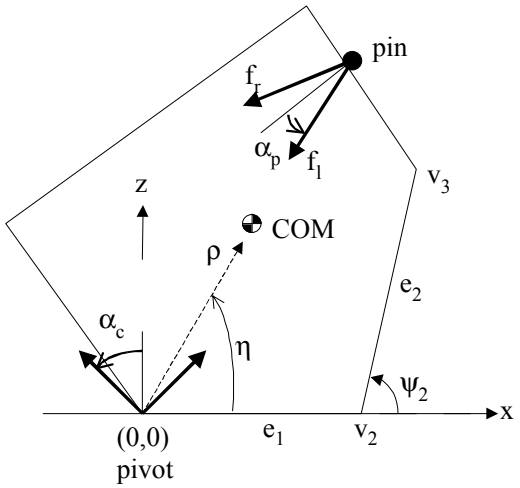

Figure 2. Notation.

Figure 2 illustrates our notation. The part moves from left to right on the conveyor belt. The conveyor friction cone half-angle is $\alpha_t = \tan^{-1}\mu_t$ and the pin friction cone half-angle is $\alpha_p = \tan^{-1}\mu_p$. The pivot point is the vertex about which the part rotates, taken to be at (0,0). The COM is a distance ρ from the origin and an angle η from the +X axis at an initial stable orientation. We denote the vector at the left edge of the pin's friction cone as f_l and the right edge as f_r.

Starting from the pivot, we consider each edge of the part in counter-clockwise order, namely e_1, e_2, …, e_n. The edge e_i, with vertices v_i at (x_i, z_i) and v_{i+1} at (x_{i+1}, z_{i+1}), is in direction ψ_i from the +X axis. The analysis given below is repeated for each stable orientation of the part.

IV. Toppling Analysis

We divide toppling into a rolling phase and a settling phase as shown in Figure 3. Let θ denote the orientation of the part from the +X axis. *Rolling* involves the rotation of the part from the initial orientation ($\theta = \theta_0$) to the unstable equilibrium orientation ($\theta = \theta_t$) where the COM is directly above the pivot. During *Settling*, the part rotates from the unstable equilibrium orientation to the next stable orientation ($\theta = \theta_1$).

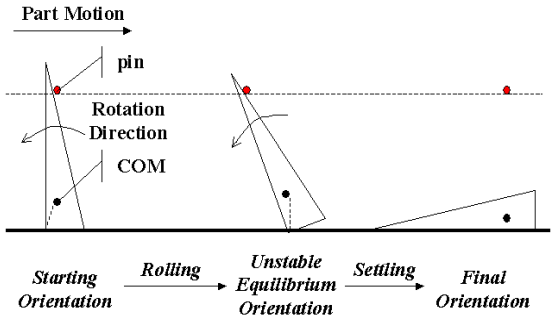

Figure 3. Two phases of toppling: *rolling and settling*.

There are four types of functions that describe critical heights as the part rotates. The radius function, $R(\theta)$, gives the height of the COM. The vertex functions, $V_i(\theta)$, give the height of vertex i and terminate when the vertex is no longer visible from +X axis. The rolling functions, $H_i(\theta)$, give minimal heights for pin contacts to initiate toppling and are determined for each edge at $\theta_0 < \theta < \theta_t$ The jamming functions, $J_i(\theta)$, give the critical height below which jamming may occur and are determined for each edge at $\theta_t < \theta < \theta_1$. All of these functions are combined to form the toppling graph.

A. Radius Function

For a polygonal part, the radius function is piecewise sinusoidal[5]. Each local minimum of corresponds to a stable orientation of the part.

B. Vertex Functions

The vertex function, $V_i(\theta) = x_i \sin\theta + z_i \cos\theta$, describes the height of vertex i as the part rotates. Like the radius function, it is piecewise sinusoidal. The vertex function is truncated after its global maximum at the point where it intersects another vertex function. This is the point at which the vertex is no longer visible from the +X axis and therefore can no longer be contacted by a pin. Figure 4 illustrates the vertex functions and the radius function for the part in Figure 2. Note that a pin at a height h contacts edge e_i if $V_i(\theta) < h < V_{i+1}(\theta)$.

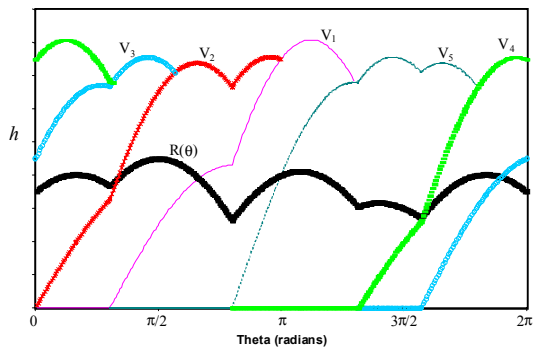

Figure 4. Radius function, $R(\theta)$, and vertex functions, $V_i(\theta)$.

C. *Rolling Functions*

During the rolling phase, the pin causes the part to rotate about its contact point with the conveyor belt surface: the *pivot point*. Friction between the part and the conveyor belt must prevent the pivot point from slipping on the belt; but friction between the part and the pin must allow the part to slip relative to the pin. Also, the system of forces on the part, including: the contact force at the conveyor, the contact force at the pin, and the part's weight, must generate a positive (counterclockwise) moment on the part about the pivot point.

The rolling function, $H_i(\theta)$, is the minimum height that the toppling contact in edge e_i must be in order to roll the part during the rolling process, where $\theta = \theta_0 \sim \theta_t$. The function is determined as a function of θ using an analysis based on Lynch's rolling conditions[1]. Those conditions extend a graphical method from Mason[24].

We begin by constructing a region as shown in Figure 5 with vertices P_1 at $(\rho \cos(\eta+\theta), \rho \cos(\eta+\theta)/\mu_t)$, P_2 at (0,0), and P_3 at $(\rho \cos(\eta+\theta), -\rho \cos(\eta+\theta)/\mu_t)$. For a fixed pin to cause rolling, the contact force between the pin and the part must make positive moment about every point in the $P_1P_2P_3$ triangle.

By examining the kinematics of the part and the pin during rotation, we can determine which direction the pin slips relative to the part. This allows us to limit our consideration to one edge of the friction cone, depending on the direction of slip. In general, the rolling conditions will depend on whether the contact has a positive or negative X coordinate, i.e. whether it is right or left of the Z-axis.

Let w_i be the distance along edge e_i as shown in Figure 5. Any point on e_i can be expressed in terms of w_i as $(x_i + w_i \cos\psi_i, y_i + w_i \sin\psi_i)$. Let w_i^* denote the critical value where the contact is on the Z-axis. Thus:

$$x_i \cos\theta - z_i \sin\theta + w_i^* \cos(\psi_i + \theta) = 0,$$

and

$$w_i^* = (-x_i \cos\theta + z_i \sin\theta)/\cos(\psi_i + \theta), \quad (1)$$

the height of the point at w_i^* is:

$$H_i^*(\theta) = x_i \sin\theta + z_i \cos\theta + w_i^* \sin(\psi_i+\theta). \quad (2)$$

The contact is left of the Z-axis if $w_i > w_i^*$; right of the Z-axis if $w_i > w_i^*$. Let $H_{il}(\theta)$ denote $H(\theta)$ when the contact is left of the Z-axis, and $H_{ir}(\theta)$ denote $H(\theta)$ when the contact is right of the Z-axis.

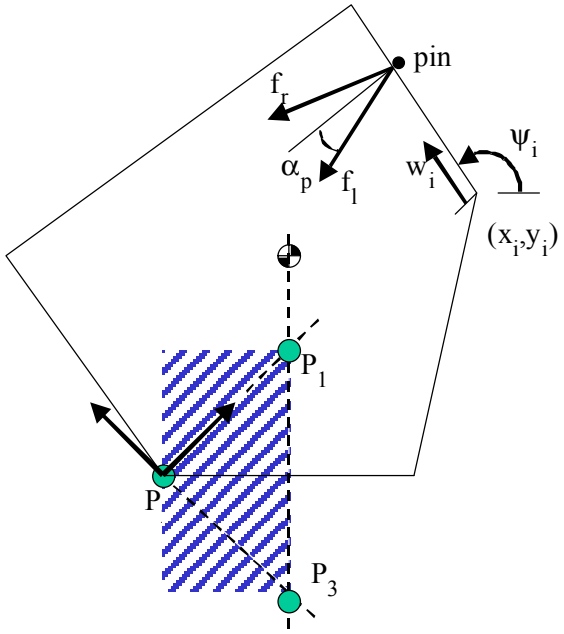

Figure 5. Conditions for the rolling phase.

1) *Contact to the right of the Z-axis*

For the case where $w_i \le w_i^*$, as the part rotates, the contact between the part and the pin moves such that w_i is decreasing. Therefore, the contact force must be at the left edge of the pin friction cone. The rolling height for this case is determined by projecting lines from P_1 and P_2 at the angle of f_l until they intersect the edge of the part. Of these two intersections, the one with the maximum height indicates the rolling height, $H_{il}(\theta)$, if it is less than $H_i^*(\theta)$.

Let ${}_lw_{il}(\theta)$ denote the pin contact on e_i where f_l passes exactly through point P_1. We can show through geometric construction that:

$${}_lw_{il}(\theta) = (2\mu_t z_i \cos\beta_{il} - \rho\cos(\beta_{il}-\eta) - \rho\cos\nu_{il} - 2\mu_t x_i \sin\beta_{il} + \mu_t \rho \sin(\beta_{il}-\eta) + \mu_t \rho \sin\nu_{il}) / (2\mu_t \sin(\beta_{il}-\psi_i)). \quad (3)$$

where $\beta_{il} = \psi_i + \pi/2 + \alpha_p$ and $v_{il} = \beta_{il} + \eta + 2\theta$.

Similarly, the contact on e_i for f_1 passing through P_2 is given by

$$ {}_2w_{il}(\theta) = (z_i \cos\beta_{il} - x_i \sin\beta_{il}) / \sin(\beta_{il} - \psi_i). \quad (4) $$

Let $w_{il}^{\#}$ denote the maximum of ${}_1w_{il}$ and ${}_2w_{il}$. By geometry, $w_{il}^{\#}$ can be shown to be

$$ w_{il}^{\#} = \begin{cases} {}_1w_{il} & 0 < \theta < \theta_{12} \\ {}_2w_{il} & \theta_{12} < \theta < \theta_2 \end{cases} \quad (5) $$

where

$$ \theta_{12} = \pi - \alpha_t - \alpha_p - \psi_i \quad (6) $$

$$ \theta_2 = \pi - \alpha_p - \psi_i \quad (7) $$

Therefore, for $w_i \le w_i^*$, the rolling function, $H_{il}(\theta)$ is given by

$$ H_{il}(\theta) = x_i \sin\theta + z_i \cos\theta + w_{il} \sin(\psi_i + \theta), \quad (8) $$

where

$$ w_{il} = \begin{cases} 0 & w_{il}^{\#} < 0 \\ w_{il}^{\#} & 0 \le w_{il}^{\#} \le w_i^* \\ w_i^* & w_{il}^{\#} > w_i^* \end{cases}. \quad (9) $$

2) Contact to the left of the Z-axis

In this case, where $w_i > w_i^*$, the contact between the part and the pin moves such that w_i is increasing. Therefore, the contact force must be at the right edge of the pin friction cone. Rolling is guaranteed if a force at the angle of the right edge of the pin friction cone generates a positive moments about the $P_1P_2P_3$ triangle.

Let ${}_1w_{ir}(\theta)$ denote the contact on e_i where f_r passes exactly through point P_1. We can show through geometric construction that:

$$ {}_1w_{ir}(\theta) = (2\mu_t z_i \cos\beta_{ir} - \rho\cos(\beta_{ir} - \eta) - \rho\cos v_{ir} - 2\mu_t x_i \sin\beta_{ir} + \mu_t \rho \sin(\beta_{ir} - \eta) + \mu_t \rho \sin v_{ir}) / (2\mu_t \sin(\beta_{ir} - \psi_i)). \quad (10) $$

where $\beta_{ir} = \psi_i + \pi/2 - \alpha_p$ and $v_{ir} = \beta_{ir} + \eta + 2\theta$.

There is no angle at which a force at f_r will pass through P_1 or P_3 and be higher than ${}_2w_{ir}(\theta)$. Therefore, for $w_i > w_i^*$, $H_{ir}(\theta)$ is given by:

$$ H_{ir}(\theta) = x_i \sin\theta + z_i \cos\theta + w_{ir} \sin(\psi_i + \theta), \quad (11) $$

where

$$ w_{ir} = \begin{cases} w_i^* & {}_1w_{ir} \le w_i^* \\ {}_1w_{ir} & w_i^* \le {}_1w_{ir} \le l_i \\ \infty & {}_1w_{ir} \ge l_i \end{cases} \quad (12) $$

and l_i is the length of edge e_i.

3) Contact on both sides of the Z-axis

If a part edge has a component to the left of the Z-axis and a component to the right of the Z-axis, there may be two separated contact regions on the edge where rolling can occur. For this reason there will be three rolling functions: $H_{il}(\theta)$ for the partial edge left of the Z-axis, $H_{ir}(\theta)$ for the partial edge right of the Z-axis, and $H_i^*(\theta)$. For this case, the pin at height h can roll the part if $H_i^*(\theta) > h > H_{ir}(\theta)$ or $h > H_{il}(\theta)$, where $\theta_i < \theta < \theta_t$.

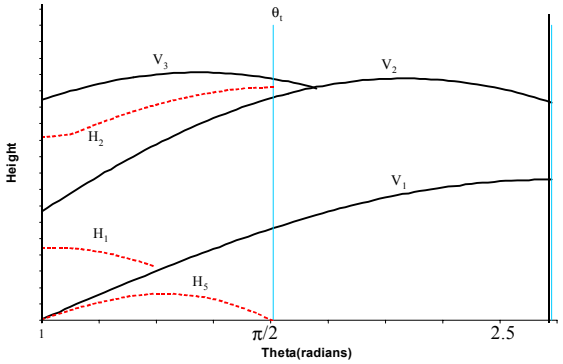

Figure 6. Rolling functions $H_{il}(\theta)$, $H_{ir}(\theta)$, and $H^*(\theta)$.

Figure 6 illustrates the functions $H_i(\theta)$ where the pivot is v_5 in Figure 2. In this case $\alpha_t = 0.65$cm, $\alpha_p = 0.09$cm, $\rho = 9$cm, and $\eta = 50°$. The kink in $H_2(\theta)$ indicates the rotational angle where ${}_2w_{2r}$ becomes higher than ${}_2w_{1r}$. We determine $H_i(\theta)$ for each visible edge of the stable orientations. Note that $H_i(\theta)$ must be bounded by the $V_i(\theta)$ and $V_{i+1}(\theta)$ and is truncated where it intersects those functions.

D. Jamming Function

After the part has rotated to θ_t, rolling phase ends and the settling phase begins. The part may jam while settling due to the friction. We must insure that the part will fall to the next stable orientation without jamming. Under our quasi-static assumptions, we do not consider the inertial dynamics (i.e., bouncing or having the part continue to rotate past its next stable orientation due to momentum).

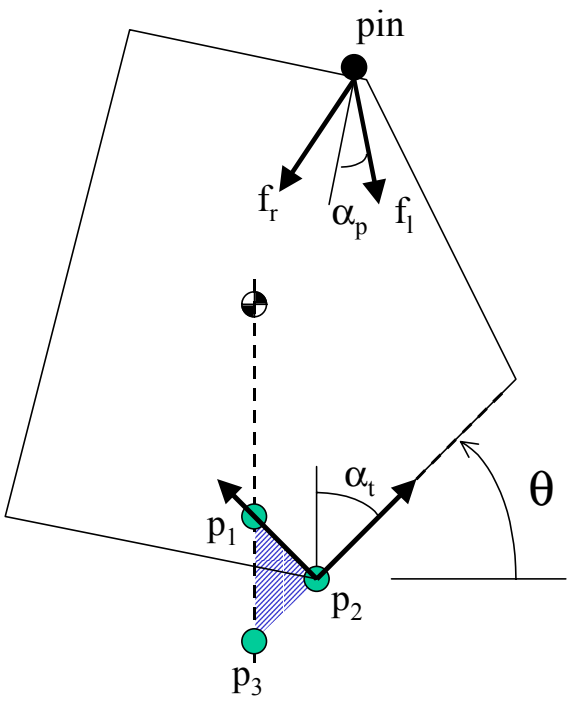

Figure 7. Jamming conditions.

Jamming is the compliment of the rolling process. For rolling all forces within the pin friction cone must make a positive moment about the $P_1P_2P_3$ triangle; to guarantee no jamming any force within the pin friction cone must not make a negative moment about $P_1P_2P_3$. Figure 7 shows that due to the position of the COM during settling the $P_1P_2P_3$ triangle is oriented in the opposite direction as during rolling. We again divide our consideration into the situations where the contact is at the left/right of Z-axis.

1) Contact to the right of the Z-axis

When the contact is right of the Z-axis, rotation causes the contact to move such that w_i is decreasing. The contact force, therefore, is at f_l. Projecting lines at the angle of the left edge of the friction cone from P_1, P_2, and P_3 until they intersect the edge, we obtain:

$$ {}_3w_{il}(\theta) = (2\mu_t z_i \cos\beta_{il} + \rho\cos(\beta_{il}-\eta) + \rho\cos\nu_{il} - 2\mu_t x_i \sin\beta_{il} + \mu_t\rho\sin(\beta_{il}-\eta) + \mu_t\rho\sin\nu_{il}) / (2\mu_t \sin(\beta_{il} - \psi_i)). \quad (13) $$

Any pin lower than the minimum of these three functions will cause jamming. Let $q_{il}^{\#}$ be the minimum of ${}_1w_{il}$, ${}_2w_{il}$, and ${}_3w_{il}$. $q_{il}^{\#}$ can be shown to be

$$ q_{il}^{\#} = \begin{cases} {}_3w_{il} & \theta_t < \theta < \theta_{32} \\ {}_2w_{il} & \theta_{32} < \theta < \theta_{21} \\ {}_1w_{il} & \theta_{21} < \theta < \pi - \psi \end{cases} \quad (14) $$

where

$$ \theta_{21} = \pi + \alpha_t - \alpha_p - \psi_i \quad (15) $$

$$ \theta_{32} = \pi - \alpha_t - \alpha_p - \psi_i \quad (16) $$

Therefore, The jamming function for this situation, $J_{il}(\theta)$, is then given by

$$ J_{il}(\theta) = x_i \sin\theta + z_i \cos\theta + q_{il}\sin(\psi_i + \theta) \quad (17) $$

where

$$ q_{il} = \begin{cases} 0 & q_{il}^{\#} \le 0 \\ q_{il}^{\#} & 0 \le q_{il}^{\#} \le w_i^* \\ w_i^* & q_{il}^{\#} > w_i^* \end{cases} \quad (18) $$

and $\theta_t < \theta < \theta_l$.

2) Contact to the left of the Z-axis

When the contact is left of the *Z*-axis, rotation causes the contact to move such that w_i is increasing. The contact force, if exists, is at f_r. In this situation it is impossible to cause jamming since f_r cannot create a negative moment about the $P_1P_2P_3$ triangle. Therefore the jamming function equals 0, i.e., $J_{ir}(\theta) = 0$, when $w_i > w_i^*$.

E. The Toppling Graph

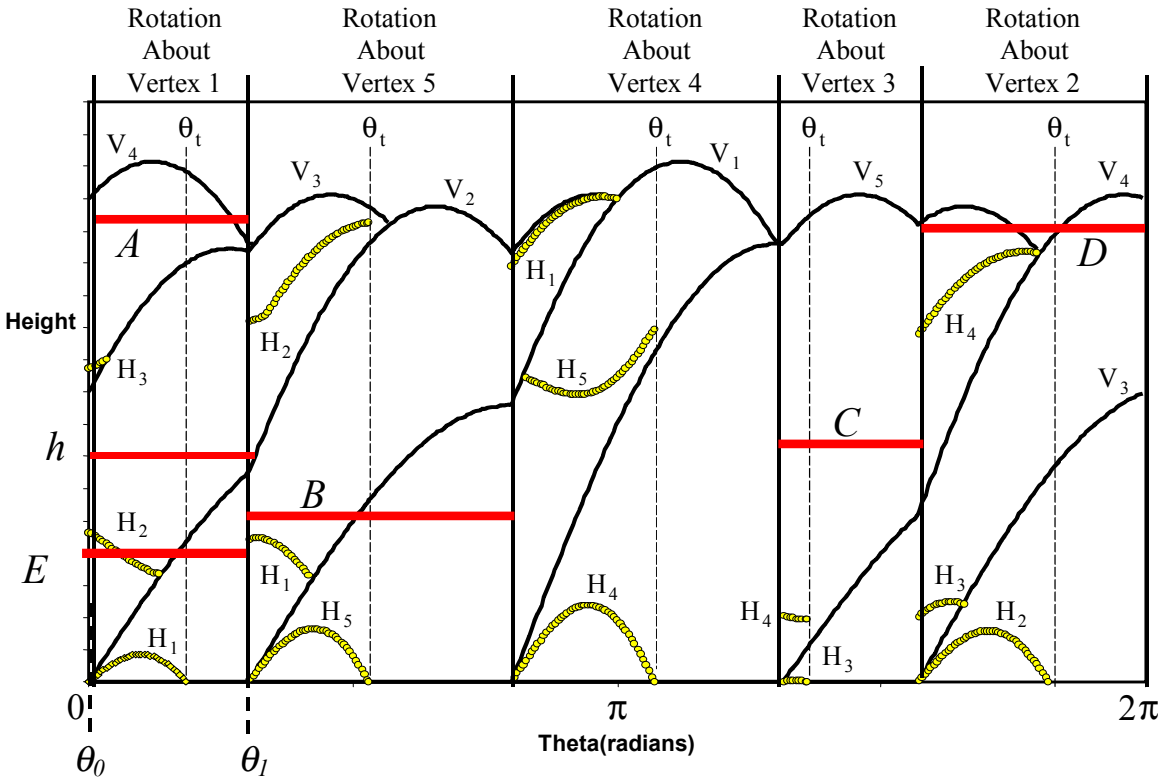

Figure 8. The toppling graph for the part in Figure 2.

Figure 8 illustrates the toppling graph which combines the radius, vertex height, rolling height, and jamming functions to represent the full mechanics of toppling. From the toppling graph the critical pin heights for each visible edge of each stable orientation can be determined or shown to be non-existent.

The toppling graph can be divided into vertical sections between each stable orientation of the part on the belt. Each section describes the rotation of the part from one stable orientation to the next stable orientation. Consider the left most section of the graph in Figure 8. The part initially is in a stable orientation with $\theta_0 = 0$. We want it to rotate about vertex 1 to the next stable orientation with $\theta_1 = 52°$. Note that H_{il} is denoted by H_i in this graph for clarity. A pin at height h will achieve this if we can draw a horizontal line corresponding to height h in the graph beginning at θ_0 and ending at θ_1 with the following characteristics:

1. if $V_i(\theta) < h < V_{i+1}(\theta)$, then $H_i^*(\theta) > h > H_{ir}(\theta)$ or $h > H_{il}(\theta)$, where $\theta_0 < \theta < \theta_t$;
2. if $V_i(\theta) < h < V_{i+1}(\theta)$, then $J_{il}(\theta) < h$, where $\theta_t < \theta < \theta_1$; and
3: $h < \max_i (V_i(\theta))$, where $\theta_0 < \theta < \theta_t$.

The first two criteria are satisfied when the pin is above both the rolling height and the jamming height on the edge it contacts. When h crosses a vertex function, the part switches contact edges and then h must be above the rolling height and jamming functions for the new edge. The third criterion is that the pin must not lose contact with the part by passing over it during the rolling phase.

Note on the graph that the solid vertical lines indicate the angles of stable orientations and the dashed vertical lines indicate different θ_t. From the graph we can determine a range of heights for each stable orientation in which a pin will topple the part to the next stable orientation, or determine the range does not exist.

The toppling graph described above predicts for each orientation of the part the *immediate action function* that takes place when the part hits a pin at a specified height. The four possible values of the function are:

- *Non-action*: the part passes under the pin or hits the pin but falls back to the same stable orientation;

- *Jamming*: the part gets stuck;
- *Repeating*: the part turns to the next stable orientation and will hit the same pin again;
- *Passing*: the part turns to the next stable orientation and will not hit the same pin again.

For example a pin at height *A* will cause Passing; while at *B* and *C* Repeating will occur. Note that *B* switches edges during rotation. *D* is an example of Non-action, where rotation begins but is not successful due to loss of contact with the part before reaching θ_t. *E* represents Jamming when the pin contacts with edge e_2.

V. Physical Experiment

We conducted a physical experiment using an Adept Flex Feeder conveyor belt. The part from Figure 2 was machined from aluminum and the pin from steel. The corresponding friction cone half angles are $\alpha_t = 53° \pm 2°$ (the belt is made from a high friction material), and $\alpha_p = 5° \pm 2°$. The critical pin heights predicted by the toppling graph are compared with physical experiment in Table 1.

Pivot Vertex	Initial Contact Edge	Critical Pin Heights (cm)	
		Prediction	Experiment
1	2	[2.9, 5.7]	[2.8, 5.7]
1	3	[8.3, 9.5]	[8.3, 9.5]
5	1	[2.6, 4.1]	[2.6, 4.1]
3	4	[1.2, 8.6]	[1.8, 8.6]
2	3	[1.5, 3.4]	[1.5, 3.4]

Table 1. Comparison of predicted pin heights with experiment using aluminum part.

Although our friction measurements are inexact, the predictions are close in all cases except the lower bound in row 4. Since we project w_i onto the vertical to find $H_i(\theta)$, errors along the edge are projected and thus reduced by the sine of the edge angle. The sine is close to 1 in the 4th row, thus this error is larger. For the upper bounds in this row, the top of the edge defines the limit in both prediction and experiment.

VI. Pin Design

As parts enter the part feeder, they can be in any stable orientation on the conveyor belt. We want to design a sequence of pin locations that will cause the part to emerge in only one final orientation. After constructing the toppling graph, the planning algorithm applies it to design such a sequence or to determine that no such sequence exists.

For each stable orientation, we compute the immediate action function. This function maps the height of the pin to four possible values: Non-action, Jamming, Passing, and Repeating. We extract this information from the toppling graph. The complexity of the immediate action function is the same as the complexity of the toppling graph: for each of the $O(n)$ stable orientations of the part, there are $O(n)$ possible intervals linked to actions.

Rather than the immediate action, we would like to know what the final outcome will be after the part interacts with a pin. Therefore we define the *final outcome function* for each stable orientation. This function maps a pin height to the index of a stable orientation, or to the value *Jamming*.

The final outcome function can be computed from the immediate action functions. For a stable orientation f_i, the Jamming intervals in the immediate action function appear as Jamming intervals in its final outcome function. The Non-action intervals map onto index *i*. The Passing intervals map onto index *i*-1 (or n+ *i*-1 if *i*-1 $\leq$ 0). The Repeating intervals map onto index *i-1*, or must be further subdivided by considering the immediate action function of the next stable orientation. This has to be repeated until either all intervals are filled in, or we cyclically reach f_i again, in which case the remaining intervals are labeled jamming (because the part will keep on rotating in front of the pin). See Figure 9 for an example.

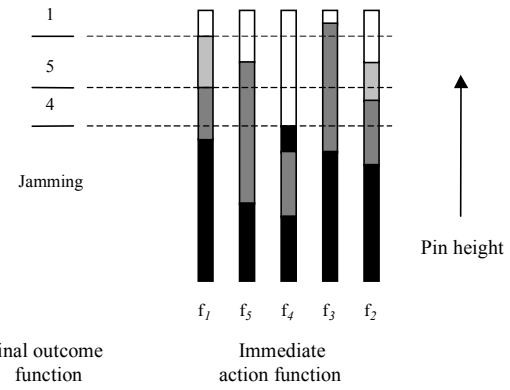

Figure 9. Pin action diagram: the computation of the final outcome function for stable orientation f_1 from the immediate action functions. The black vertical bars correspond to Jamming; the heavy shaded bars to Repeating; the light shaded bars to Passing; and the white bars to Non-action.

Because every interval boundary is a boundary in one of the immediate action functions, the complexity of the final outcome function is $O(n^2)$. We need such a function for each of the $O(n)$ stable orientations.

The final outcome function provides the basis for the pin design algorithm. Initially the part can be at any stable orientation. After passing a pin, the part can still lie on a subset of the stable orientations. Clearly, the height of the pin should be such that it never jams the part. So, it must lie outside of the union of the jamming intervals of all final outcome functions. By merging the final outcome functions, we derive $O(n^3)$ different intervals of pin heights which each maps our set of all possible stable orientations onto (smaller) sets of stable orientations.

For each of the smaller sets we repeat the process of merging the final outcome functions, to compute height intervals for the second pin together with the corresponding, again smaller, sets of stable orientations. We continue until we reach a set of cardinality one (or sets can no longer be reduced). In this way we can compute the smallest set of pins required to uniquely orient the part.

In the worst case, this design algorithm can take exponential time, $O(n^{3n})$. We are studying properties of the action functions that will yield an algorithm with better asymptotic complexity.

VII. Discussion and Future Work

We have studied how industrial parts can be fed (oriented) using a sequence of fixed horizontal pins to reorient them as they move past on a conveyor belt. We defined the *toppling graph*, a new data structure that explicitly represents the mechanics of toppling, rolling, and jamming. Given the n-sided convex polygonal projection of a part, its center of mass and frictional coefficients, we described an $O(n^2)$ algorithm to compute the toppling graph and verified its predictions with a physical experiment. We then describe an $O(n^{3n})$ pin design algorithm that uses the toppling graph to design a sequence of pin locations that will cause the part to emerge in a unique orientation or to determine that no such sequence exists.

Our pin height analysis is greatly simplified when friction with the conveyor belt is infinite and friction with the pin is zero (approximated when the conveyor belt is of high friction and the pins are implemented with freely rotating bearings). This shrinks the $P_1P_2P_3$ triangle to a line segment with the pivot point as the critical point. This also merges $H_i(\theta)$ and $J_i(\theta)$ into a single continuous function. $H_i(\theta)$ is minimized in all cases and the increase in $J_i(\theta)$ due to the increase in conveyor friction is balanced by the decreased ability of the pin to cause jamming.

For cases where no pin sequences exists, we can consider introducing a wiper, an angled pin that guides the part at particular orientations to fall off the conveyor belt or another orienting device such as a step[22] or ramp. We are currently[25,26] extending the toppling analysis to the design of self-aligning jaws for a parallel-jaw gripper as shown in Figure 10.

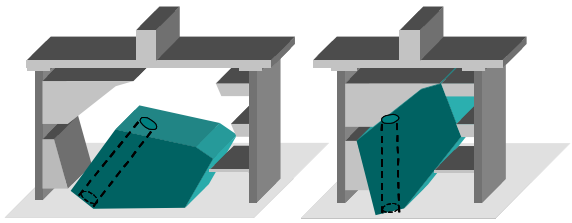

Figure 10. A parallel-jaw gripper can rotate the part from its initial resting orientation into a desired assembly orientation as it is grasped.

Acknowledgements

We would like to thank Kevin Lynch for his elegant toppling analysis and ongoing feedback. This work was supported in part by the National Science Foundation under CDA-9726389, Presidential Faculty Fellow Award IRI-9553197, and NATO Collaborative Research Grant CRG 951224. Berretty was supported by the Dutch Organization for Scientific Research (N.W.O.).

References

[1] K. Lynch. Toppling Manipulation. In *IEEE International Conference on Robotics and Automation*, Vol.4, p.2551-7, Detroit, MI, May 1999.

[2] K. Lynch. Inexpensive Conveyor-Based Parts Feeding. *Assembly Automation*, Vol. 19, No. 3, p. 209-15, 1999.

[3] M. A. Erdmann and M. T. Mason. An Exploration of Sensorless Manipulation. *IEEE Journal of Robotics and Automation*, Vol. 4, No. 4, p.369-79, August, 1988.

[4] R. C. Brost. Dynamic Analysis of Planar Manipulation Tasks. In *IEEE International Conference on Robotics and Automation*, Vol.3, p.2247-54, Nice, France, May 1992.

[5] K. Goldberg. Orienting polygonal parts without sensors. *Algorithmica*, Vol.10, No. 2, p.201-25, August, 1993. Special Issue on Computational Robotics.

[6] T. Abell and M. Erdmann. Stably Supported Rotations of a Planar Polygon with Two Frictionless Contacts. In *IEEE/RSJ International Conference on Intelligent Robots and Systems*, Vol.3, p.411-18, Pittsburgh, PA, August 1995.

[7] N. Zumel and M. Erdmann. Nonprehensile Two Palm Manipulation with Non-Equilibrium Transitions between Stable States. In *IEEE International Conference on Robotics and Automation*, Vol.4, p.3317-23, Minneapolis, MN, April 1996.

[8] N. Zumel and M. Erdmann. Nonprehensile Manipulation for Orienting Parts in the Plane. In *IEEE International Conference on Robotics and Automation*, Vol.3, p.2433-9, Albuquerque, NM, April 1997.

[9] T. Lozano-Perez. Motion Planning and the Design of Orienting Devices for Vibratory Part Feeders. MIT AI Lab Technical Report. January 1986.

[10] B. K. Natarajan. Some Paradigms for the Automated Design of Part Feeders. *International Journal of Robotics Research*, Vol. 8, No. 6, p.98-109, December 1989.

[11] M. Caine. The Design of Shape Interactions Using Motion Constraints. In *IEEE International Conference on Intelligent Robots and Systems*, Vol. 1, pp. 366-71, 1994.

[12] A. Christiansen, A. D. Edwards, and C. A. C. Coello. Automated Design of Part Feeders Using a Genetic Algorithm. In *IEEE International Conference on Robotics and Automation*, Minneapolis, Vol.1, p.846-51, MN, April, 1996.

[13] D. R. Berkowitz and J. Canny. Designing Parts Feeders Using Dynamic Simulation. In *IEEE International Conference on Robotics and Automation*, Vol.2, p.1127-32, Minneapolis, MN, April, 1996.

[14] M. A. Peshkin and A. C. Sanderson. Planning robotic manipulation strategies for workpieces that slide. *IEEE Journal of Robotics and Automation*, Vol.4, No.5, p.524-31, October, 1988.

[15] J. Wiegley, K. Goldberg, M. Peshkin, and M. Brokowski. A Complete Algorithm for Designing Passive Fences to Orient Parts. In *IEEE International Conference on Robotics and Automation*, Vol.1, p.550-556, 1998.

[16] R-P Berretty, K. Goldberg, M. H. Overmars, and A. F. Stappen. On Fence Design and the Complexity of Push Plans for Orienting Parts. In *13th ACM Symposium on Computational Geometry,* p.21-9, June, 1997.

[17] D. Gudmundsson and K. Goldberg. Tuning Robotic Part Feeder Parameters to Maximize Throughput. *Assembly Automation*, Vol. 19, No. 3, p.216-21, 1999.

[18] S. Akella, W. Huang, K. Lynch, and M. Mason. "Parts feeding on a conveyor with a one joint robot," *Algorithmica*, Vol.26, No.3-4, p.313-344, 2000.

[19] A. Bicchi and R. Sorrentino. Dexterous Manipulation through Rolling. In *IEEE International Conference on Robotics and Automation*, Vol.1, p.452-457, 1995.

[20] R.-P. Berretty, K. Goldberg, L. Cheung, M. Overmars, G. Smith, and A. Stappen. Trap Design for Vibratory Bowl Feeders. In *IEEE International Conference on Robotics and Automation*, Vol.4, p.2558-63, Detroit, MI, May 1999.

[21] S. Blind, C. McCullough, S. Akella, and J. Ponce. "A Reconfigurable Parts Feeder with an Array of Pin," In *IEEE International Conference on Robotics and Automation*, Vol.1, p.147-153, San Francisco, 2000.

[22] R. Zhang and K. Gupta. Automatic Orienting of Polyhedral through Step Devices. In *IEEE International Conference on Robotics and Automation*, Vol.1, p.550-556, 1998.

[23] Y. Yu, K. Fukuda and S. Tsujio. Estimation of Mass and Center of Mass of Graspless and Shape-Unknown Object. In *IEEE International Conference on Robotics and Automation*, Vol.4, p.2893-8, Detroit, MI, May 1999.

[24] M. T. Mason. Two Graphical Methods for Planar Contact Problems. In *IEEE/RSJ International Workshop on Intelligent Robots and Systems*, p.443-8, Osaka, Japan, November 1991.

[25] T. Zhang, G. Smith and K. Goldberg. Compensatory Grasping with the Parallel Jaw Gripper. In *Algorithmic and Computational Robotics: New Directions*, edited by B. Donald, K. Lynch, and D. Rus, p.169-80, A K Peters, Ltd., 2001.

[26] T. Zhang and K. Goldberg. Design of Gripper Jaws Based on Trapezoidal Modules. In *IEEE International Conference on Robotics and Automation*, Seoul, Korea, 2001.